This manuscript is prepared for submission to the Journal of Geophysical Research for publication.

IN SITU STRESS DETERMINATION IN THE DEVONIAN SHALES (IRA McCOY 20402) WITHIN THE ROME BASIN

by

C. E. Brechtel
A. S. Abou-Sayed
Terra Tek, Inc.

and

R. J. Clifton
Brown University

Submitted to

Columbia Gas System Service Corporation
1600 Dublin Road
Columbus, Ohio 43215

Attn: Edward J. Ranostaj

Submitted by

Terra Tek, Inc.
University Research Park
420 Wakara Way
Salt Lake City, Utah 84108

TR 76-36
July 1976

ABSTRACT

The *in situ* stress field was determined at a depth of 837 m (2,745 feet) in Devonian shale ("gray" shale) within the Rome Basin in West Virginia. Logging data and laboratory observations of core samples reveal vertical cracks oriented at N 50° - 60° E. Because of these cracks and their preferred orientation, a new approach based on fracture-mechanics concepts is used to evaluate the *in situ* stresses from the field and laboratory data. The resulting prediction of the maximum horizontal stress is compared to that predicted by Haimson and Fairhurst's (1967) method; the latter overestimates the value of the stress because the effect of loading the faces of any pre-existing crack had been neglected.

The results of the field experiment are summarized as follows:

Breakdown Pressure = P_b = 20.2 MPa (2930 psi);

Shut-in Pressure = P_s = 16.3 MPa (2360 psi);

Bearing of Fracture = N 45° E to N 55° E.

The analysis of the results gives the following values of the *in situ* principal stresses:

Overburden Stress = σ_{OB} = 22.1 MPa (3210 psi), vertical;

Maximum Horizontal Stress = σ_{HMAX} = 21.6 MPa (3130 psi), horizontal, N45° E to N 50°E;

Mininum Horizontal Stress = σ_{HMIN} = 16.3 MPa (2360 psi), horizontal, N 40° W to N 45° W.

This page intentionally left blank.

TABLE OF CONTENTS

This page intentionally left blank.

LIST OF ILLUSTRATIONS

This page intentionally left blank.

LIST OF TABLES

This page intentionally left blank.

INTRODUCTION

Recent attempts to stimulate natural gas production in low-permeability sandstones in the Western United States by massive hydraulic fracturing (MHF) have resulted in increases of flow of up to 8 times (J. Wroble, Pacific Transmission Supply Co., 1976). However, many attempts have been unsuccessful, probably owing to certain unfavorable characteristics of the pay formations, such as permeability, pore pressure and deformation moduli (Randolph, 1976), all of which are affected by the magnitude of the *in situ* stress. Thus, knowledge of the stress state in the pay and surrounding formations is essential in the simulation of *in situ* conditions during laboratory experiments designed to measure the true characteristics. These measurements, in turn, make the analysis of such phenomena as containment of the frac within the pay zone and *in situ* permeability more reliable. In addition, determination of the *in situ* state of stress at depth gives insight into what will be the breakdown pressure, extension pressure, and the direction of fracture during MHF. The difference in horizontal principal stresses is of particular interest because the direction of a hydraulic fracture will be determined by the principal stress direction if the difference in principal stresses is significantly greater than local fluctuations in principal stresses. Furthermore, knowledge of the direction of the minimum *in situ* principal stress and/or the preferred orientation of natural fracture systems is needed in deviated-well technology (Komar, 1976-a). There, the well bore is drilled at a predetermined inclination with its horizontal projection aligned with either the direction of minimum *in situ* principal stress or orthogonal to the direction of the natural fracture system.

Field techniques to determine the magnitudes and directions of *in situ* principal stresses include, among others, mini-hydrofracturing. The method is a by-product of the hydraulic fracture stimulation technique. The conventional analysis of the results of mini-hydrofracturing involves computation of the *in situ* stresses from the elasticity solution for a pressurized, smooth, well bore in an isotropic, homogeneous elastic medium.

During a mini-hydrofracturing experiment to determine *in situ* stresses in the Devonian shales within the Rome Basin of West Virginia, it was observed that the natural fractures in the core samples from the test well, (Ira McCoy 20402), violated the assumptions used in the conventional methods of calculating the *in situ* stress field (cf. Haimson and Fairhurst, 1967). The problem was therefore approached using the principles of linear elastic fracture mechanics, and the results of this analysis suggest that the conventional analysis is partially incorrect. The error occurs because the mechanics of fracture initiation and fracture extension are ignored in the conventional method of calculating *in situ* stress from the elasticity solution for a pressurized cylindrical cavity.

As a result of the problems encountered in applying the conventional method of calculating the *in situ* stress field in this test, the present report has been divided into two distinct sections. The first section deals with the conventional approach as applied to this particular experiment; the stress field determined by these calculations indicates the inconsistency and non-uniqueness that can arise in an extreme case. A proposed new approach is presented in the second section. The differences between the

in situ fields obtained by the two approaches are due mainly to loading of pre-existing cracks by the frac fluid. From fracture mechanics such loading has a marked effect on crack extension and should therefore be considered.

This page intentionally left blank.

THE OPEN-HOLE FIELD TESTS AND RESULTS

Background

Mini-hydrofracturing follows procedures similar to those used in MHF; however, the hole is left open so that the orientation of the fracture can be determined after the formation has been broken. Its application is potentially* unlimited in depth, and does not depend upon the determination of load-deformation response, as in the case of overcoring techniques. Since its inception, it has undergone theoretical development (cf. Hubbert and Willis, 1957, Kehle, 1964 and Haimson and Fairhurst, 1967) and has been applied in both laboratory (Lamont and Jessen, 1963 and Haimson and Fairhurst, 1967) and field experiments in Rangely, Colorado (Raleigh, *et al.*, 1972) at a depth of 1920m (6300 ft.) and in the Rainier Mesa at the Nevada Test Site (Haimson, *et al.*, 1973) at depths up to 270 m (880 ft.). The experimental procedures used in a mini-hydrofracturing experiment are described in detail elsewhere (Haimson, 1968); therefore, only a brief description of the techniques will be presented here.

The section of the hole to be tested is isolated by lowering "straddle packers" into position and then pressurizing the sealing components at each end of the device (see Figure 1). The "fracturing fluid" is then injected into the section between the upper and lower seals. Surface and, if possible, downhole recorders are used for continuously monitoring the fluid pressure. The pressure is raised slowly until the breakdown pressure (P_b) is reached, i.e., the pressure at which the rock surrounding the hole fractures. If the flow rate remains constant after the breakdown pressure has been reached, the pressure will drop to a constant level, known as the extension pressure

* Depth limitation comes from unavailability of pumping equipment suitable for the necessary high pressure needed for great depths.

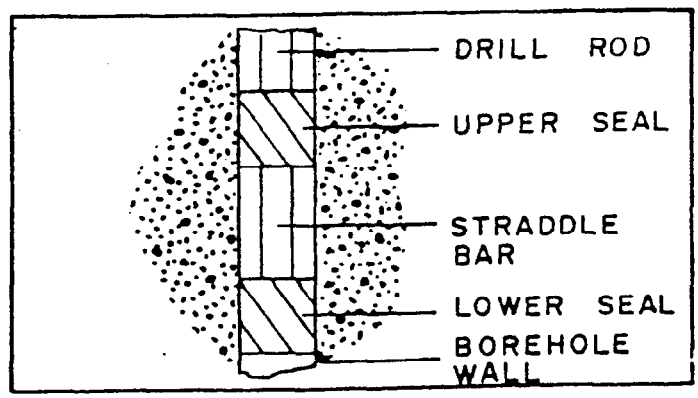

Figure 1. Configuration of a typical straddle packer.

(P_f) at which the fracture propagates. If the fluid-flow is stopped, the entire system will come to an equilibrium where the *in situ* stress acting to close the fracture equals the fluid pressure; this equilibrium pressure is the shut-in pressure (P_s). Finally, to determine the orientation of the fracture, an impression packer is lowered into the test section and a trace is formed on the packer by extruding a soft rubber membrane into the fracture. A photograph of a downhole compass is taken and then correlated with a reference mark on the outside of the packer.

Results of the Open-Hole Test

The open-hole test was conducted using a standard Lynes straddle packer for a 22.2 cm (8-3/4 inch) hole. The straddle length was roughly 4.27 m (14 feet) and its center was located at a depth of 837 m (2745 ft). The packer and drill stem were then filled with fluid, a combination of KCl, Macobar Drispak, and water, which was used to drill the well. The packers were then pressurized to 10.5 MPa (1520 psi, downhole gage).

After the packer had been pressure-set, the formation was pressurized until the breakdown pressure was reached (see Figure 2). Both the pressure and flow rate were monitored at the surface and a downhole pressure monitor

installed in the straddle bar confirmed the surface measurements. Figure 3 indicates the breakdown of the formation and the initial extension of the fracture in more detail. It was not possible to record the instantaneous shut-in pressure after breakdown because a pressure fitting at the top of the drill stem started leaking.

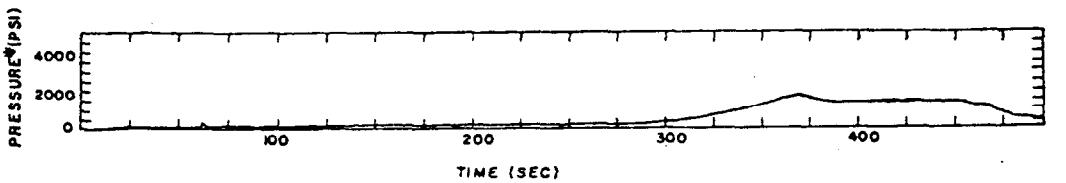

Figure 2. Test record indicating breakdown pressure and extension pressure.

* Add hydrostatic head equal to 8.4 MPa (1220 psi).

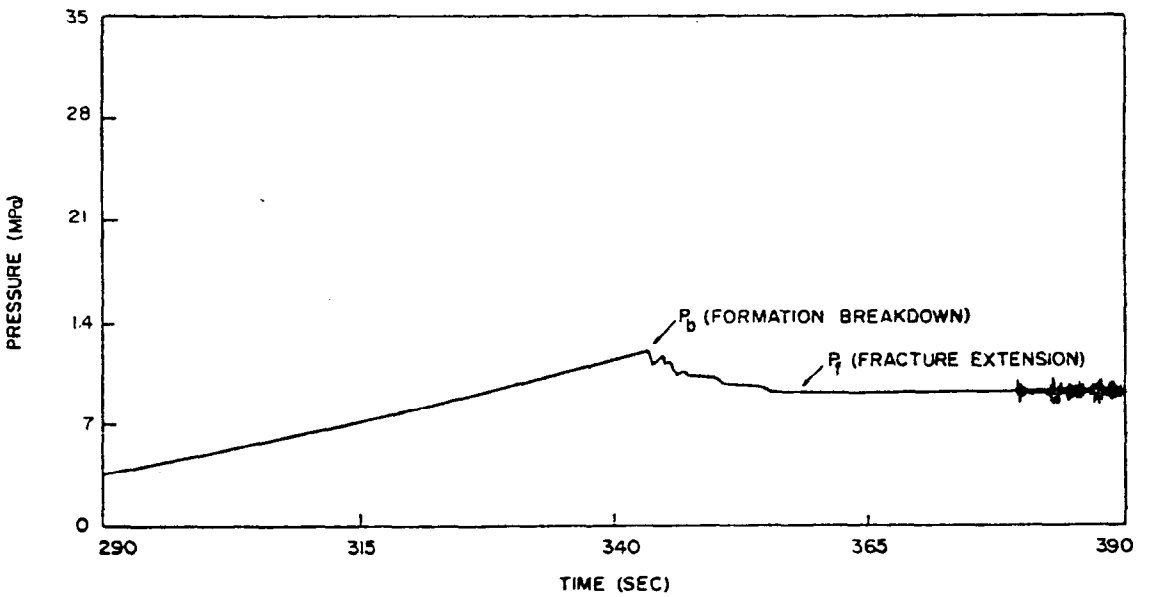

Figure 3. Test record indicating breakdown pressure and extension pressure.

* Add hydrostatic head equal to 8.4 MPa (1220 psi).

The pressure fitting was replaced and the shut-in pressure was measured on the two successive runs, shown as Figures 4 and 5.

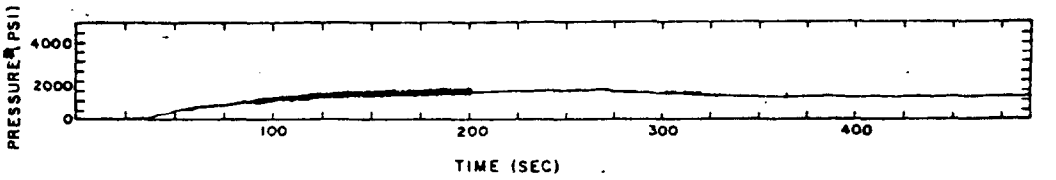

Figure 4. Fracture extension and shut-in Number 1.
* Add hydrostatic head equal to 8.4 MPa (1220 psi).

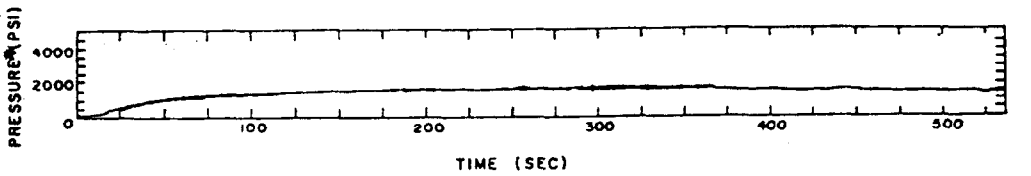

Figure 5. Fracture extension and shut-in Number 2.
* Add hydrostatic head equal to 8.4 MPa (1220 psi).

The numerical results of the open-hole test are presented below in Table I. Maximum variation between the successive measurements of the shut-in pressure was within ± 6 percent.

TABLE I
Results of the Open-Hole Test

Pressure Run	Breakdown Pressure (P_b) Mpa (psi)	Shut-in Pressure (P_s) Mpa (psi)
1	20.2 (2930)	---
2	---	16.4 (2380)
3	---	17.3 (2470)
4	---	15.3 (2215)

The straddle packer was removed from the hole and a Lynes impression packer was lowered to map the fracture that had been formed. The bottom of the impression was at 839 m (2752 feet); it extended 3.66 m (12 ft.) with

a 0.61 m (2 ft.) blank in the middle. The impression packer indicated the formation of a very narrow, vertical fracture over its entire length. The bearing of the fracture trace at the borehole surface was determined to be N 45° E to N 50° E by using an Eastman Whipstock single-shot, downhole camera.

Evaluation of the *In Situ* Stress Field

Determination of the complete *in situ* stress field can be achieved if the three principal stresses and their directions can be calculated. In general, several mini-hydrofracturing experiments in non-coplanar boreholes are required to obtain the necessary information. This method was used to measure the *in situ* stress at the Nevada Test Site (Haimson, *et al.*, 1973). If, however, the direction and magnitude of one of the principal stresses are know, the complexity of the experimental work needed to determine the other two principal stresses is reduced substantially. This situation is not uncommon since the vertical (overburden) stress is usually a principal stress and, except at very shallow depth, will generally exceed the minimum *in situ* stress. Under these circumstances, the fracture plane will be vertical, and a single mini-hydrofracturing experiment is sufficient to estimate the directions and magnitudes of the horizontal *in situ* principal stresses.

If the rock is viewed as a homogeneous, isotropic, elastic medium with an isotropic failure criterion, it is easily shown that a crack propagating in this medium due to fluid pressure acting on its face will grow along the path of least resistance (i.e., it will extend in the plane perpendicular to the least compressive *in situ* principal stress). For a moderately long crack, the pressure required to hold the crack open, but not extend it, will be slightly greater than the far-field stress acting normal to the fracture.

Therefore, it follows that the shut-in pressure is approximately equal to the minimum horizontal compressive stress.

In this case, if the rock is assumed to fail when a critical tensile stress is reached then the principal stress field can be calculated by applying Equations (1), (2) and (3)

$$\sigma_{HMAX} = T_o + 3P_s - P_b - P_o \quad (1)$$

$$\sigma_{OB} = \gamma H \quad (2)$$

$$\sigma_{HMIN} = P_s \quad (3)$$

where σ_{HMAX}, σ_{HMIN} and σ_{OB} are total principal stresses and

γ = specific weight of rock

H = depth of the test zone

P_o = formation pore pressure

T_o = tensile strength of the rock

P_s = shut-in pressure

P_b = breakdown pressure

This solution, based on the elasticity solution for a pressurized cylindrical cavity in an infinite isotropic elastic continuum, was first proposed by Hubbert and Willis, (1957) and Haimson and Fairhurst, (1967). It should be noted that Equations (1) and (3) are valid only for the case where the fracturing fluid does not penetrate the matrix of the formation material. Due to the low permeability of the Devonian shales of the Rome Basin, neglect of fracturing-fluid penetration should not introduce major errors into the analysis. Equations (1), (2) and (3) are not applicable if the vertical stress is less than the smallest horizontal stress, in which case a horizontal fracture will form and determination of the horizontal *in situ*

principal stresses is not possible using the mini-hydrofracturing technique.

In addition to the magnitude of the *in situ* principal stresses obtained from the measured pressures and Equations (1) and (3), the impression packer provides the direction of the cracks that have formed at the borehole wall. If the material is isotropic, these cracks should be normal to the direction of the minimum principal stress.

Results of the Laboratory Experiments

Laboratory tests conducted in this study were used to supply the material properties necessary to obtain the *in situ* stresses from the field test. A series of six hollow-cylinder burst tests were conducted on oriented core samples recovered from the Gray-Shale section at a depth of 823 m (2699 ft.) to 845 m (2770 ft.). These tests, when interpreted in terms of a critical tensile stress required for fracture, provided the tensile strength (T_o) of the shale. A description of the experimental techniques used in these tests can be found elsewhere (Haimson and Fairhurst, 1967).

Briefly, the test consists of internal pressurization of a thick-walled cylindrical sample until failure occurs. The failure pressure, P_i, is measured and is related to the tensile strength of the rock, T_o, through the equation

$$T_o = P_i\left(\frac{w^2 + 1}{w^2 - 1}\right) \tag{4}$$

where w is the ratio of the outer radius b to the inner radius a of the hollow cylinder.

In spite of the visual competence of the shale from the test section, nearly all of the core samples developed extensive horizontal fractures during transportation to the Terra-Tek facility. The fractures are apparently

due to bedding-plane separation caused by the removal of the overburden stress. These fractures limited the length of the burst-test specimens to less than 63 mm (2.5 in). The results of these laboratory tests are shown in Table II.

TABLE II
Results of Unjacketed Burst-Tests

Sample Depth m (ft.)	b/a = w	P_i Failure Pressure MPa (psi)	Remarks
823 (2699)	10.7	22.3 (3230)	Very competent sample, few fractures.
831 (2724)	10.7	7.7 (1120)	Failed on pre-existing fractures.
836 (2741)	10.7	11.3 (1640)	Failed on pre-existing fractures.
836.3 (2742)	10.7	2.3 (340)	Failed along a bedding-plane fracture.
842 (2761)	10.7	5.9 (850)	Failed along a bedding-plane fracture.
845 (2770)	10.7	19.2 (2790)	Very competent sample, very few fractures.

It is obvious that the results from the unjacketed burst test can be grouped into two classes. Samples at 823 m and 845 m level have an average tensile strength which is over twice as great as for samples at the 831 m and 836 m levels. Samples from depths of 823 m and 845 m had considerably fewer natural fractures than the samples from the 831 m and 836 m levels. Both of the samples that failed at the lower pressures (831 m and 836 m) had groups of small, tight fractures with the same directional trend, and the failure plane induced during the test was parallel to the pre-existing fractures. The pressure required to fail samples from 823 m and 845 m appear to be representative of the tensile strength of the matrix material, while the

lower values (831 m and 836 m) appear to be pressures required to extend a pre-existing natural fracture.

Calculation of *In Situ* Stress Assuming an Elastic, Isotropic Medium

A comparison of the densities obtained from the Birdwell 3-D ultrasonic log and the density measurements done by Terra Tek indicates excellent agreement. Therefore, the log densities were averaged and used to calculate the overburden stress. The calculated value for the overburden stress σ_{OB} is 22.1 MPa (2310 psi).

The tensile strengths used in the calculations of the horizontal stresses are an average of the two values in each group shown in Table II. The three measurements of the shut-in pressure were averaged to determine the value of the minimum horizontal stress, σ_{HMIN}. The pore-pressure term in Equation (1) is estimated, based on downhole pressure build up test, to be 1.7 MPa (250 psi) (Smith, 1976). A tabulation of the measured and calculated data at the mid-position of the fractured section (837 m) is presented in Table III.

TABLE III

Calculation of *In Situ* Stress for an Elastic Isotropic Media

Depth M (feet)	P_b MPa (psi)	P_o MPa (psi)	P_s MPa (psi)	T_{oavg} MPa (psi)	γ KPa/m (psi/ft)	$\sigma_{OB} = \gamma H$ MPa (psi)	$\sigma_{HMAX} = T_o + 3P_s - P_b - P_o$ MPa (psi)	$\sigma_{HMIN} = P_s$ MPa (psi)	Direction of σ_{HMAX}
837 m (2745 ft)	20.2 (2930)	1.7 (250)	16.3 (2360)	21.1 (3060)	26.4 (168.5)	22.1 (3210)	48.1 (6980)	16.3 (2355)	N45°-50°E
837 m (2745 ft)	20.2 (2930)	1.7 (250)	16.3 (2360)	9.7 (1400)	26.4 (168.5)	22.1 (3210)	36.7 (5300)	16.3 (2355)	N45°-50°E

As a result of the two types of behavior observed in the laboratory tests, it is not possible to arrive at a unique value for the minimum horizontal stress. If the material in the test section, between the packers, was isotropic and homogeneous with a tensile strength of 21.1 MPa (3060 psi), then a maximum horizontal stress of 48.1 MPa (6980 psi) would be obtained.

However, if the tensile strength of the rock was 9.7 MPa (1400 psi) the maximum horizontal stress would be 36.7 MPa (5300 psi).

The wide range of measured burst pressures coupled with the effect of the known existing fractures observed in the recovered cores indicate that the shale medium has a pronounced anisotropy with respect to its tensile strength. Figure 6 shows that the induced failure plane is parallel to the group of existing fractures in the sample at the 831 m (2726 ft) level. Furthermore, examination of the fracture-density logs from the nearby well, Ira McCoy 20403, indicates a consistent set of fractures through the entire cored section (see Figure 7) whose azimuths are within ± 10 degrees of the direction of the fracture created during the mini-hydrofracturing test. Hence, the assumption of an isotropic critical-tensile-strength failure criterion is not satisfied.

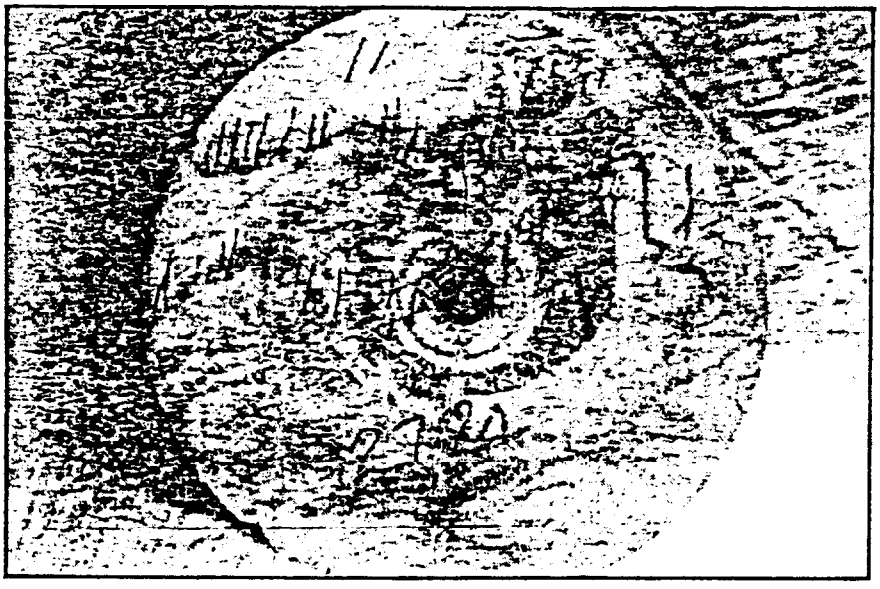

Figure 6. Burst sample from 831 m (2724 ft.) [P_i = 7.7 MPa (1120 psi)].

In order to account for the existence of the developed fracture system in the field test, the problem has been reanalyzed by applying the methods of linear elastic fracture mechanics. The effect of preferred crack orientation on fracture growth and the initiation of fracture on a pre-existing crack are accounted for in the calculation of the *in situ* stress. The calculated stress field will be found to differ from the estimates obtained using the conventional formulation (Haimson and Fairhurst, 1967).

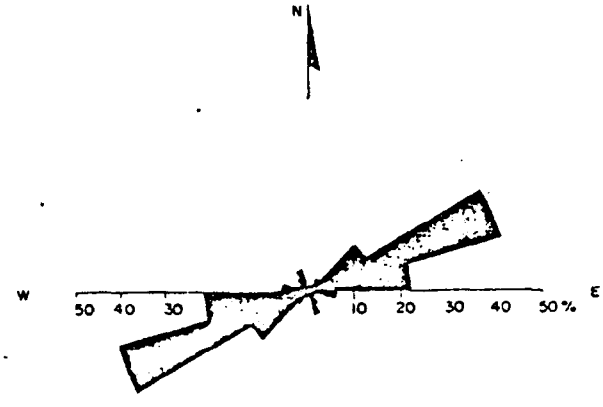

Figure 7. Histogram of the strikes of 605 vertical extension fractures mapped in Devonian Shale recovered from well No. 20403 (from Swolfs, *et al.*, 1976).

This page intentionally left blank.

FRACTURE-MECHANICS ANALYSIS OF THE MINI-HYDRAULIC FRACTURE TEST

Growth of a crack inclined to the directions of the far-field *in situ* stresses, and subjected to pressure on its faces can be analyzed by using fracture mechanics concepts in which linear elasticity is assumed and attention is given to the elevation of stresses near the crack tip. While large stresses around the crack tip will usually be accompanied by some plasticity, linear elastic fracture mechanics properly forms the basis for analyses when the plastic zone and other non-linear effects around the crack tip will be confined to a small region within a linear elastic field. Such a field is characterized by a single parameter. Irwin (1960) introduced the stress-intensity factor K as one such parameter--others include the J-integral (Rice, 1968) and the specific energy-release rate, G (Irwin, 1957). These parameters, which are equivalent in linear elastic fracture mechanics, measure the intensity of the local stress field at the crack tip. They are determined by the applied loading. Cracks are expected to advance if the values of these parameters reach critical values characteristic of the material considered. On the other hand if the loads acting on the body and its geometry are such that the value of K, J, or G is less than this material property, the crack is expected to remain stationary.

Effect of Preferred Crack Orientation on Crack Growth in Hydraulic Fracturing

Consider a pressurized crack oriented at an arbitrary angle α relative to the direction of minimum principal stress σ_3 of the far-field stress system, illustrated in Figure 8. If the crack faces of length 2L are subjected to a pressure p, the stress-intensity factors K_I and K_{II} for the existing crack are given by (cf. Rice, 1970, eq. 97):

$$K_I \doteq \sqrt{\pi L}\ \{p - \sigma_1 \sin^2\alpha - \sigma_3 \cos^2\alpha\} \tag{5}$$

$$K_{II} = \sqrt{\pi L}\ \{\tfrac{1}{2}(\sigma_1 - \sigma_3) \sin 2\alpha\} \tag{6}$$

where $\sigma_1 = \sigma_{HMAX} > \sigma_3 = \sigma_{HMIN}$ denotes the maximum compressive far-field horizontal principal stress.

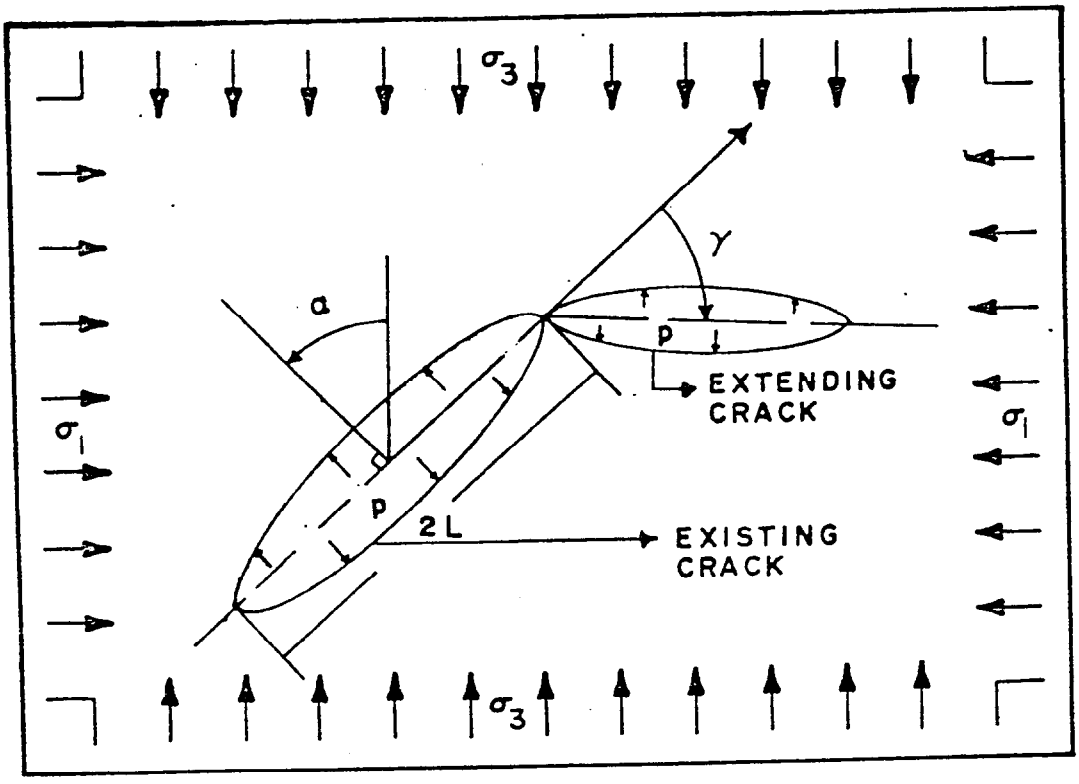

Figure 8. Skewed crack under far-field stress and internal pressure.

If the existing crack extends in an arbitrary direction, as shown in Figure 8, then the energy-release rate $\Gamma(\gamma)$ associated with extension in the direction γ will be given by the following equation (Hussain, *et al.*, 1974)

$$\Gamma(\gamma) = \frac{4(1-\nu^2)}{E}\left(\frac{1}{3+\cos^2\gamma}\right)\left(\frac{\pi-\gamma}{\pi+\gamma}\right)^{\gamma/\pi}\left[(1+3\cos^2\gamma)K_I^2 + 8\sin\gamma\cos\gamma K_I K_{II} + (9-5\cos^2\gamma)K_{II}^2\right] \quad (7)$$

where K_I and K_{II} are given by equations (5) and (6), and E and ν denote the Young's modulus and Poisson's ratio of the material, respectively. If the crack is assumed to advance in the direction, γ_{max}, for which $\Gamma(\gamma)$ is a maximum, then the relationship between the direction of crack advance, γ_{max}, and the ratio, (K_{II}/K_I), is given by Figure 9 (Clifton, 1974).

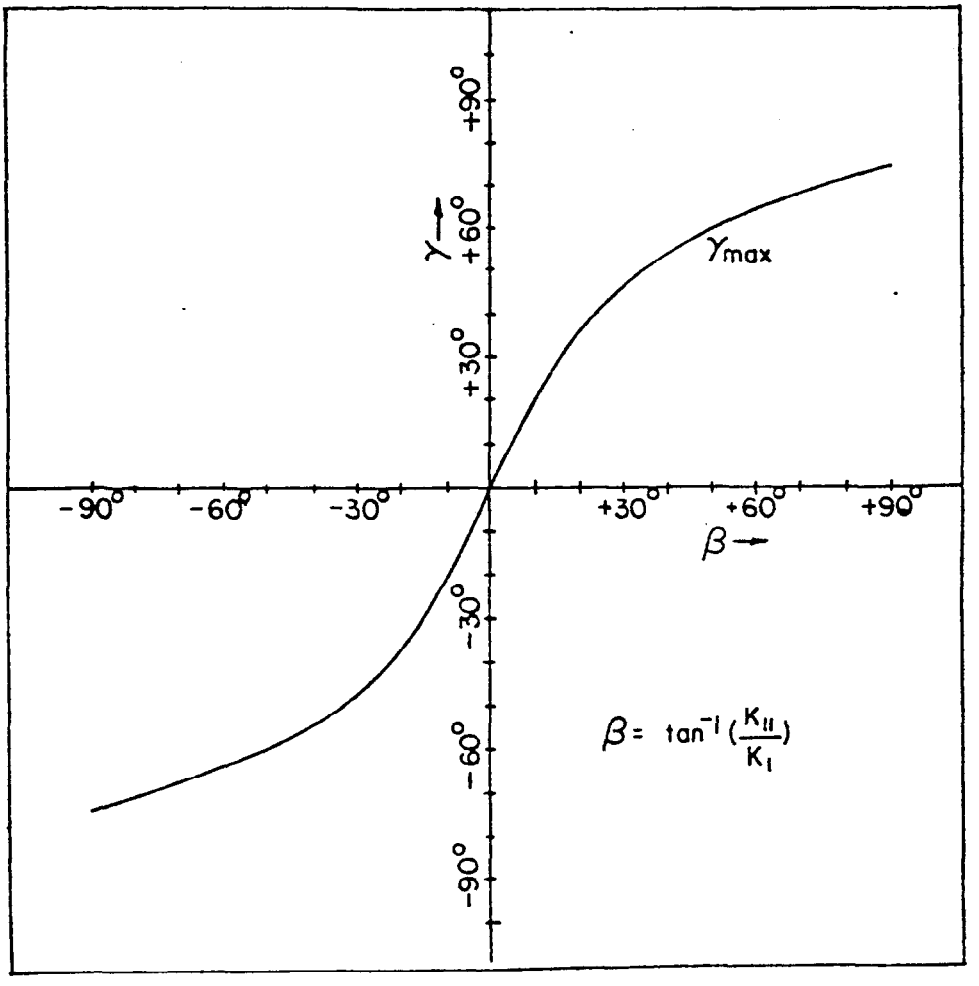

Figure 9. Orientation of propagating crack which maximizes energy-release rate (Clifton, 1974).

When K_I and K_{II} are substituted from equations (5) and (6) into the expression (7), $\Gamma(\gamma)$ is found to be proportional to the crack length and a positive definite function of K_I and K_{II}. Therefore, if cracks advance for a prescribed finite value of $\Gamma(\gamma_{max})$, the only way a long open crack can be stationary is for K_I and K_{II} to be equal to zero. Thus, long cracks are stationary only for (assuming that the crack faces are not in contact)

$$p = \sigma_1 \sin^2\alpha + \sigma_3\cos^2\alpha \tag{8a}$$

and

$$(\sigma_1 - \sigma_3) \sin 2\alpha = 0 \tag{8b}$$

If σ_1 and σ_3 are not equal, Equation (8b) requires that

$$\alpha = 0 \quad \text{or} \quad \alpha = \pi/2$$

In the former case, $\alpha = 0$, the pressure p equals the minimum horizontal compressive stresses σ_3, whereas in the latter case, $\alpha = \pi/2$, the pressure p equals the maximum horizontal compressive stress σ_1. That is, long open cracks can be stationary only if they are parallel to principal-stress directions and if the pressure p is equal to the principal stress perpendicular to the crack face. Whether the case $\alpha = \pi/2$ or $\alpha = 0$ is more likely to occur can be determined by noting whether an arbitrarily oriented crack tends to rotate to become perpendicular to σ_1 or to σ_3. From Figure 8, the value of γ for which $\Gamma(\gamma)$ is a maximum has the same sign as β. And, for $K_I > 0$, β has the same sign as K_{II}. Then, for $(\sigma_1 - \sigma_3) > 0$, equation (5) implies that $K_{II} > 0$ for $\alpha < \pi/2$. Therefore, γ is positive for α in the range $[0, \pi/2]$. In other words, the crack tends to extend in a direction which is more nearly perpendicular to the direction of minimum compressive stress than was the existing crack as long as $(\sigma_1 - \sigma_3)$ is not zero.

As a result, the pressure in the long crack approaches the minimum compressive stress σ_3. Hence, for moderately long cracks, the shut-in pressure, P_s, is given by

$$P_s = \sigma_3 = \sigma_{HMIN} \tag{9}$$

Equation (9) confirms the use of (3) for determining the minimum *in situ* stress. An estimate of the maximum horizontal *in situ* stress, $\sigma_{HMAX} = \sigma_1$, can be obtained by considering the initial advance of an existing crack which intersects the bore hole at a prescribed orientation.

Crack Initiation with a Pre-Existing Crack of Prescribed Orientation

Consider the cylindrical hole with two radially opposed cracks subjected to an internal pressure p and the far-field stress state σ_1 and σ_3 as shown in Figure 10.

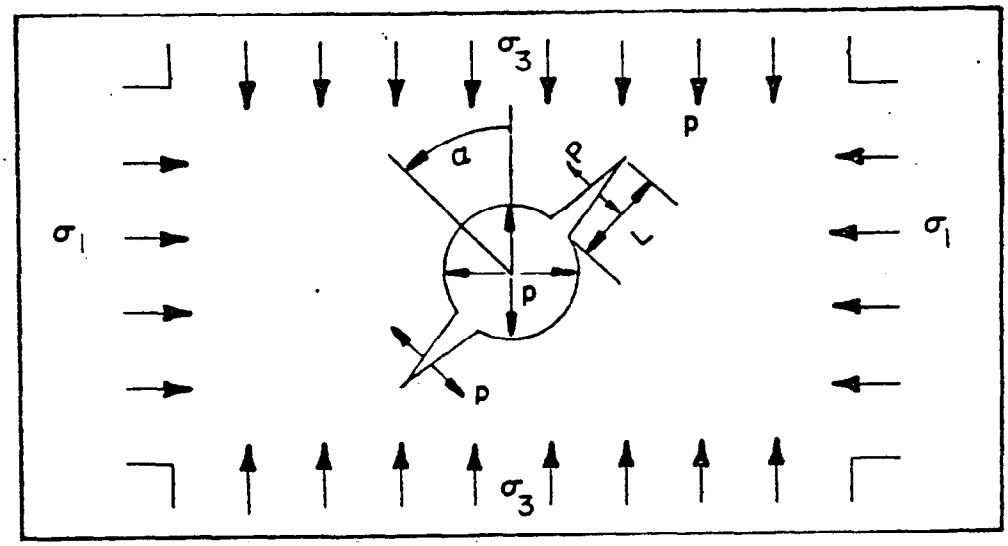

Figure 10. Crack in a bore-hole wall under far-field stress and internal pressure.

The stress-intensity factor, K_I, at the crack tip is given by (Johnson, *et al.*, 1973, Eq. 49)

$$K_I = -p\sqrt{L\pi}\ F(L/a) - (\sigma_1 \cos^2\alpha + \sigma_3 \sin^2\alpha)\ F(L/a)\ \sqrt{L\pi}$$

$$+ (\sigma_1 \cos 2\alpha - \sigma_3 \cos 2\alpha)\ G(L/a)\ \sqrt{L\pi} \qquad (10)$$

where F(L/a) and G(L/a) are given in Table A2 (cf., Paris and Sih, 1965).

In order to determine σ_1 from (10) it is necessary to know the minimum compressive stress σ_3, the initial crack length L, and the breakdown pressure $p = P_b$ at which the stress-intensity factor K_I is equal to the critical value, K_{Ic}, required for crack advance. Now σ_3 can be determined from measurement of the shut-in pressure, P_s (see (9)), and K_{Ic} can be determined from fracture toughness tests (see appendix). Estimates of L can be obtained from visual inspection of cores and from the pressure at which pre-existing cracks in hollow test cylinders begin to propagate under loading by internal pressure. For given values of K_{Ic}, P_b and L, equation (10) becomes a relation between σ_1 and α. This relation can be written in the more useful form

$$I(\alpha)(\sigma_1-\sigma_3) = \sigma_3 - P_b + \frac{K_{Ic}}{F(L/a)\sqrt{L\pi}} \qquad (11)$$

where

$$I(\alpha) \equiv \cos^2\alpha - \frac{G(L/a)}{F(L/a)} \cos 2\alpha \qquad (12)$$

The function $I(\alpha)$ is shown in Figure 11 for various values of the ratio L/a. Because $I(\alpha)$ is near zero only for a limited range of values of α it appears that (11) can usually be solved uniquely for $(\sigma_1-\sigma_3)$ when α is known.

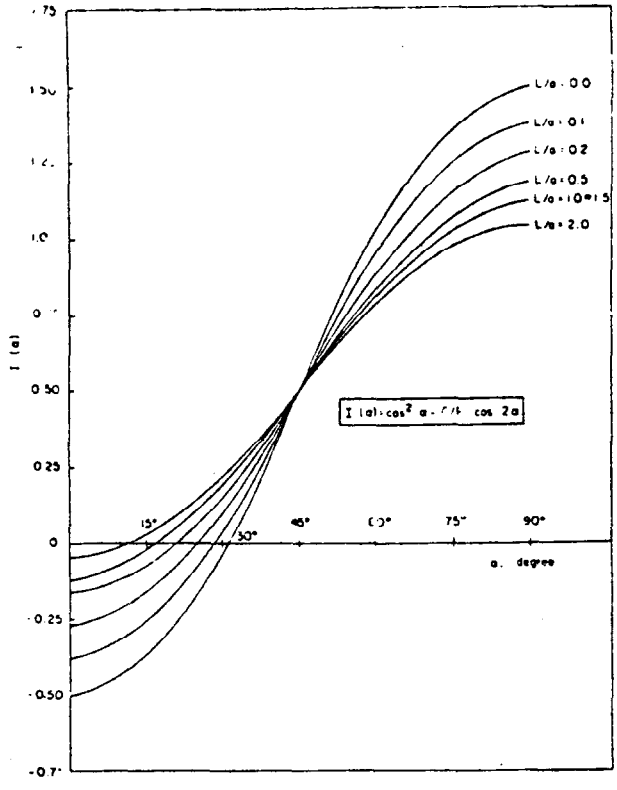

Figure 11. $I(\alpha)$ as a function of α for different ratios of (L/a)

If $\sigma_1 = \sigma_3$ then the value of α is irrelevant and the principal stresses in the horizontal plane are

$$\sigma_1 = \sigma_3 = P_b - \frac{K_{Ic}}{F(L/a)\sqrt{L\pi}} \quad . \tag{13}$$

On the other hand, the condition $\sigma_3 < \sigma_1$ requires that σ_3 and α satisfy the inequalities

$$\sigma_3 < P_b - \frac{K_{Ic}}{F(L/a)\sqrt{L\pi}} \qquad \text{for } \alpha > \alpha_c \tag{14a}$$

$$\sigma_3 > P_b - \frac{K_{Ic}}{F(L/a)\sqrt{L\pi}} \qquad \text{for } \alpha < \alpha_c \tag{14b}$$

where α_c is the solution of the equation

$$I(\alpha) = 0 \tag{15}$$

Values of α_c for a wide range of values of (L/a) (i.e., $0 \leq L/a \leq 2$) lie in the interval $15° < \alpha_c < 30°$. For known values of σ_3, P_b, K_{Ic} and L, inequalities (14) limit the possible range of the values of α. Unfortunately, however, L is generally not known with much certainty and allowable variations in the value for L may lead to satisfaction of either (14a) or (14b). Such uncertainty could be removed if a dominant crack of known depth L could be introduced in the field test.

While it appears that there is no unambiguous way of determining σ_1 without additional information, there are a number of observations that can be made. First, if cracks of known depth L could be introduced for mini-hydraulic fracturing of a well bore at two different depths within nominally the same formation, then the principal stress σ_1 could be determined without *a priori* determination of α. This would be accomplished by introducing the cracks at orientations differing by $\pi/2$ and making use of the identity $I(\alpha) + I(\alpha+\pi/2) = -1$. Then, from (11)

$$\sigma_1 = P_b^{\alpha} + P_b^{\alpha + \pi/2} - \sigma_3 - \frac{2K_{Ic}}{F(L/a)\sqrt{L\pi}} \tag{16}$$

where P_b^{α} and $P_b^{\alpha + \pi/2}$ are the breakdown pressures in the sections with cracks oriented at angles α and $\alpha + \pi/2$ respectively. Once σ_1 is obtained from (16), the angle α can be obtained from application of (11) to the results of each field test. Comparison of the two values of α obtained in this way would serve as a check on the validity of the procedure for determining σ_1 and α.

If results from only a single mini-hydrofracturing test are available, then an additional assumption must be introduced in order to estimate σ_1, unless the principal stress directions can be determined from an independent measurement of the hydraulic-fracture orientation at large distances from the well bore. In the latter case measurement of crack orientation at the well bore by means of an impression packer suffices for the determination of α. If there is no preferred orientation of existing flaws, then the expected value for α is $\alpha = 0$ because K_I is a maximum for $\alpha = 0$. On the other hand, even if there is a preferred orientation of existing cracks the development of these cracks may be such that their orientation will be near $\alpha = 0$. Such orientation would result if the cracks are due to extensional failure, i.e., lie in the principal plane of the greatest and intermediate stresses (Swolfs, *et al.*, 1976). In the Devonian-Shale core samples the existing vertical cracks are not planar and do not contain pulverized material which would suggest their formation or subsequent sliding in a shear mode. Thus, it appears plausible that initial crack extension in the mini hydraulic fracturing experiment occurs in a direction near $\alpha = 0$. Furthermore, equation (14b), measured values of P_s, P_b, K_{Ic} and laboratory values for L suggest that α satisfies $\alpha<\alpha_c$. Consequently, in what follows the orientation of the crack at the well bore will be assumed to be $\alpha = 0$. This assumption is the same as the one used in the conventional method for determining σ_{HMAX} discussed previously; use of the same assumption here facilitates direct comparison of the two approaches.

If one assumes that during a mini-hydrofracture test the initial crack intersects the borehole in a radial plane perpencidular to the minimum

in situ compressive stress, then, from (11) and (9) one obtains

$$\sigma_1 = \frac{K_{Ic}}{\sqrt{\pi L}(G-F)} - \frac{F}{(G-F)} P_b + \frac{G}{(G-F)} P_s \qquad (17)$$

where G and F are to be evaluated for appropriate values of L/a. The critical stress-intensity factor K_{Ic} is obtained from jacketed pre-notched burst tests as discussed in the Appendix. One estimate of the crack length L can be obtained from the results of the unjacketed burst tests and the value for K_{Ic} determined from the jacketed tests. Interpretation of the unjacketed burst tests in terms of linear elastic fracture mechanics gives

$$K_{Ic} = \sqrt{\pi L_o}\, P_i \hat{F}(L_o/a_o) \qquad (18)$$

where L_o and a_o are, respectively, the length of the crack and the bore radius of the cylindrical burst sample. The pressure P_i is the internal pressure at which the cylinder bursts. The function $\hat{F}(L_o/a_o)$ is a dimensionless stress-intensity factor analogous to F(L/a), but applicable to the case of finite-diameter cylinders (see Appendix). For values of L_o which are small relative to the wall thickness of the cylinder the function $\hat{F}(L_o/a_o)$ is given approximately by (Clifton, *et al.*, 1976)

$$\hat{F}(L_o/a_o) = \frac{2.26w^2}{(w^2-1)} \qquad (19)^*$$

where w = b/a is the ratio of inner and outer radii of the test cylinders. From (18), (19) and values of K_{Ic} and P_i obtained from cores taken from the section of the well pressurized by the straddle packer, the largest pre-existing vertical crack intersecting the bore in the unjacketed burst

---

* Lack of agreement between (19) and Equation (5) of Ref. (Clifton, *et al.*, 1976) is due to a misprint in the latter equation.

tests reported in Table II is L_o = 0.7 mm (.030 in). This value is obtained for K_{Ic} = 38.2 MPa $\sqrt{mm}$ (1100 psi $\sqrt{in}$) and P_i = 11.3 MPa (1640 psi), corresponding to the sample from a depth of 836 m which failed along pre-existing vertical cracks. This length is considerably less than the length of 8 mm, say, of most pre-existing vertical cracks observed in the test cores (see e.g. Figure 6). Two possible explanations of this discrepancy appear plausible. One is that the computed effective length should have been larger because $\hat{F}$ in Equation (18) was taken to be the value for a radial plane-strain crack in the limit as $L_o/a_o \to 0$. Actually $\hat{F}$ should be obtained from a three-dimensional-elasticity solution for a crack (or group of cracks) of finite extent intersecting the bore. The actual value of $\hat{F}$ is smaller than the value obtained from (19) so that use of (19) in (18) tends to underestimate L_o. The extent of this underestimate is difficult to assess, but comparison of plane-strain-crack solutions with solutions for a circular crack in an infinite medium (Sneddon, 1946), and elliptical crack in a plate (Rice and Levy, 1970) or hollow cylinder (Underwood, 1972) suggests that the stress intensity factor could be reduced by approximately 40 percent from the value for a plane-strain crack of the same depth. From (18) such a reduction in $\hat{F}$ would cause the computed value of L_o to increase to 1.2 mm (.05 in).

A second and more important reason for the discrepancy between computed and observed values for L_o is based on the fact that when a drilled hole intersects a pre-existing crack only part of the crack remains in the surrounding material after the central core is removed. Thus, the length of the remaining crack intersecting the bore is generally less than the length of pre-existing cracks, especially when the bore diameter is comparable to the crack length as in the case of the burst sample shown in Figure 6.

The considerations mentioned in connection with the determination of L_o should also be taken into account in the computation of σ_1 from (17). In the first term it appears reasonable to take the length L to be approximately equal to the length of the pre-existing cracks because many such cracks can be expected to intersect the 22.2 cm hole and it is likely that for at least one of these cracks the depth is essentially equal to the initial length of the crack. The dimensionless stress-intensity factors F and G should be reduced because the cracks are not plane-strain cracks. However, F and G should decrease similarly so that quotients F/(G-F) and G/(G-F) should be essentially the same as for plane-strain conditions. The quantity (G-F) can be expected to be approximately 40 percent less than for plane-strain conditions. Then, from (17), the maximum horizontal compressive principal stress $\sigma_{HMAX} = \sigma_1$ is approximately

$$\sigma_1 \simeq \frac{38.2}{\sqrt{\pi 8}\ (2.93 - 2.06)\ .60} - \frac{2.06}{.87}\ (20.2) + \frac{2.93}{.87}\ (16.3)$$

or

$$\sigma_1 \simeq + 14.5 - 47.8 + 54.9$$

or

$$\sigma_{HMAX} = \sigma_1 \simeq 21.6 \text{ MPa } (3130 \text{ psi}) \qquad (20)$$

The intermediate steps are shown in order to indicate the relative magnitude of the terms. The accuracy in the computed value of σ_{HMAX} is reduced because the computation involves differences in terms of comparable magnitude. However, the two large terms are regarded as known with quite good certainty (say ± 5 percent) and the larger percent error (say ± 50 percent) occurs in the smallest term. As a result, the probable error in the computed value of σ_{HMAX} is regarded as less than 30 percent. Because the computed value of σ_{HMAX} is only one-third larger than σ_{HMIN} it appears that the overall general conclusion

is that the horizontal principal stresses are not markedly different as would be inferred from the conventional method of analysis which neglects fracture mechanics. This general conclusion may have important implications for hydraulic fracturing in the Rome Basin because it suggests that at least locally, the direction of hydraulic fractures may not be well defined by principal stress directions, but may be governed by the orientation of planes of weakness.

Comparison of Two Methods for Computing σ_{HMAX}

So far, two methods for computing σ_{HMAX} have been discussed. The first, based on a critical tensile stress fracture criterion and neglect of consideration of cracks in the wall of the laboratory specimen and the field well, gives [from (1) and (4)]

$$\sigma^{t}_{HMAX} = 3P_s - P_b + \left(\frac{w^2+1}{w^2-1}\right) P_i - P_o \quad . \tag{21}$$

The second, based on linear elastic fracture mechanics gives

$$\sigma^{f}_{HMAX} = \frac{G}{(G-F)} P_s - \frac{F}{(G-F)} P_b + \frac{\hat{F}(L_o/a_o)}{(G-F)} \sqrt{\frac{L_o}{L}}\, P_i \tag{22}$$

where (18) has been used to express K_{Ic} in (17) in terms of L_o and P_i. For both (21) and (22) failure is assumed to occur on the radial plane perpendicular to the minimum *in situ* compressive stress.

If L/a and L_o/a_o are much less than unity, say less than 0.1, then (21) and (22) can be compared by considering the limiting case $L/a \to 0$, $L_o/a_o \to 0$. In this case $G = 1.5F$ and $\hat{F}(0) = (w^2/(w^2-1))F$ so that (22) reduces to

$$\sigma^{f}_{HMAX} = 3P_s - 2P_b + \frac{2w^2}{(w^2-1)} \sqrt{\frac{L_o}{L}}\, P_i \quad . \tag{23}$$

Then, for the limiting case of cracks which are small relative to radii a_o and a, the difference $\sigma^t_{HMAX} - \sigma^f_{HMAX}$ becomes

$$\sigma^t_{HMAX} - \sigma^f_{HMAX} \approx P_b - \left(\frac{2w^2}{(w^2-1)} \sqrt{\frac{L_o}{L}} - \frac{w^2+1}{(w^2-1)} \right) P_i - P_o \quad . \qquad (24)$$

For samples generally used in the laboratory burst tests the ratio w = b/a is much greater than unity so that $w^2 >> 1$ and (24) reduces to

$$\sigma^t_{HMAX} - \sigma^f_{HMAX} \approx P_b - (2\sqrt{\frac{L_o}{L}} - 1)\, P_i - P_o \quad . \qquad (25)$$

Therefore, for given P_b, P_o and P_i the difference $(\sigma^t_{HMAX} - \sigma^f_{HMAX})$ is largest (smallest) when the term $(2\sqrt{L_o/L} - 1)$ is smallest (largest). Because it is unlikely that the largest crack in the well bore is smaller than the largest crack in the bore of the laboratory specimen, an upper bound on $(2\sqrt{L_o/L} - 1)$ is +1 obtained for $L_o/L = 1$. A lower bound is -1, obtained for $L_o/L \to 0$. Using these bounds one obtained from (25) the following bounds for $(\sigma^t_{HMAX} - \sigma^f_{HMAX})$

$$P_b - P_o - P_i \leq (\sigma^t_{HMAX} - \sigma^f_{HMAX}) \leq P_b - P_o + P_i \quad . \qquad (26)$$

The breakdown pressure P_b is usually greater than the internal pressure P_i required to burst the laboratory samples so that σ^t_{HMAX} is usually greater than σ^f_{HMAX}. If P_i is small relative to $P_b - P_o$, as may be expected in the determination of σ_{HMAX} at large depths or in weak rocks, then the difference between σ^t_{HMAX} and σ^f_{HMAX} is approximately equal to $P_b - P_o$. In any event, equation (26) indicates that the two approaches lead to pronounced differences in calculated values of σ_{HMAX}.

From Table II, the pressure P_i for a burst test on a sample which was taken from the interval pressurized by the straddle packer, and which did not fail along a bedding plane, is 11.3 MPa (1640 psi). Then, for P_b = 20.2

MPa (2930 psi), P_i = 11.3 MPa (1640 psi) and P_o = 1.7 MPa (250 psi), the bounds on $(\sigma^t_{HMAX} - \sigma^f_{HMAX})$ based on (26) are

$$7.2 \text{ MPa (1040 psi)} \leq \sigma^t_{HMAX} - \sigma^f_{HMAX} \leq 29.8 \text{ MPa (4320 psi)} \quad . \quad (27)$$

The actual difference $(\sigma^t_{HMAX} - \sigma^f_{HMAX})$ based on the calculation of σ^t_{HMAX} from (21) and the value of σ^f_{HMAX} obtained from (17) with L = 8 mm is

$$\sigma^t_{HMAX} - \sigma^f_{HMAX} = 38.5 - 21.6 = 16.9 \text{ MPa (2450 psi)} \quad (28)$$

Clearly, from both (27) and (28) the two approaches lead to marked differences in the calculated values of σ_{HMAX}.

Finally, the calculated values of the principal *in situ* stresses based on the present analysis are summarized in Table IV along with other relevant parameters.

TABLE IV

The *In Situ* Stress at 837 m (2745 feet)

Depth (h) m (feet)	P_b MPa (psi)	P_s MPa (psi)	γ Kg/m³ (lbs/ft³)	L mm (in.)	σ_{OB} (Vertical) MPa (psi)	σ_{HMAX} MPa (psi)	σ_{HMIN} MPa (psi)	Direction of σ_{HMAX}
837 (2745)	20.2 (2930)	16.3 (2355)	2643 (168.5)	8	22.1 (3210)	21.6 (3130)	16.3 (2360)	N 45° - 50° E

This page intentionally left blank.

CONCLUSIONS

The fracture logs obtained from the Energy Research and Development Administration (Komar, 1976; Swolfs, *et al.*, 1976) indicate that one of the sets of natural fractures is aligned with the direction of σ_{HMAX} reported here, and support the assumption that the small flaw that was propagated during the field test was in the direction of σ_{HMAX}. Furthermore, a fracture-mechanics analysis of mini-hydrofracturing indicates that as a fracture propagates it will be oriented normal to the minimum *in situ* stress. The shut-in pressure (P_s) therefore appears to provide an accurate estimate of the minimum principal stress. Confirmation of the realignment of cracks along planes normal to the least compression has been demonstrated experimentally by Ingraffea and Heuze (1976) using a PMMA plate containing an elliptical notch and subjected to biaxial loading at its edges. They found that the crack (initially inclined to the direction of the applied stresses) turns around as it propagates and aligns itself normal to the maximum tension (minimum compression) load. These conclusions are identical to Haimson's assumptions (1968).

Because the actual crack length in the wellbore must be estimated, there exists some uncertainty in the calculation of σ_{HMAX}. The effect of the initial crack length on σ_{HMAX} is shown in Figure 12. Figure 12 indicates that the maximum value that the crack length could have, in this case, is 27 mm (1.05 in.). At this point, the horizontal principal stresses would be equal and the direction of fracture would depend only on the orientation of the physical flaws in the rock.

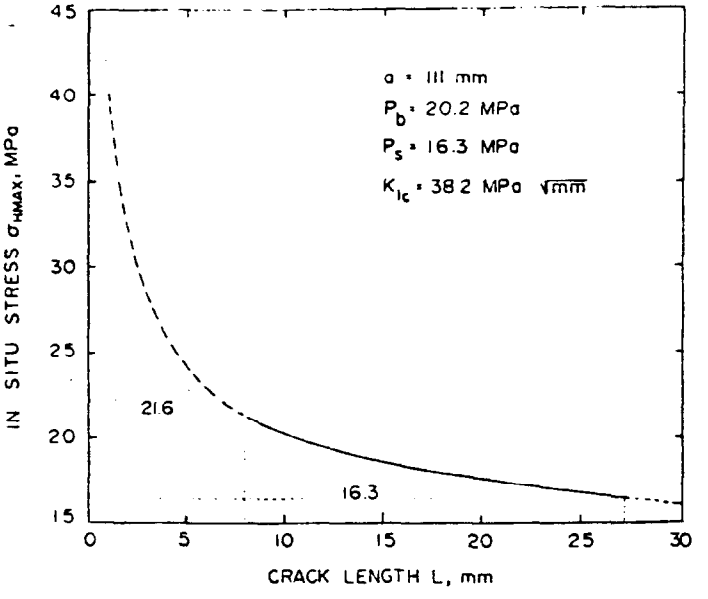

Figure 12. Variation of σ_{HMAX} for increasing crack length.

Field tests have been performed in areas surrounding the Rome Basin. Results of a mini-hydrofracturing test conducted in Falls Township, Ohio by Overbey and Rough (1968), indicate a minimum horizontal stress of 14.7 MPa (2140) psi with the fracture plane along the N 64° E direction. Another mini-hydrofracturing experiment conducted near Bradford, Pennsylvania, gives the direction of the fracture plane as N 70° E, (Overbey and Rough, 1968). Overcoring experiments conducted in a belt from northeastern Ohio through Northwestern Pennsylvania and New York place the trend of σ_{HMAX} at N 78° E, N 90° E, and N 55° E, respectively. These experiments show that σ_{HMAX} tends to be aligned with the axis of the Applachian Mountain Belt, and this corresponds fairly well with the direction indicated by the impression packer used at Ira McCoy 20402 (N 45° E to N 50° E).

REFERENCES

Bowie, O. L. and Freese, D. E., "Elastic Analysis for Radial Crack in a Circular Ring," *Eng. Fracture Mech.*, Vol. 4, p. 315, 1972.

Clifton, R. J., Simonson, E. R., Jones, A. H. and Green, S. J., "Determination of the Critical Stress Intensity Factor K_{Ic} in a Circular Ring," *Experimental Mechanics*, Vol. 16, p. 233, 1976.

Clifton, R. J., "Some Recent Developments in Fracture Mechanics," *Terra Tek Report* TR 73-70, November, 1974.

Haimson, B. and Fairhurst, C., "Initiation and Extension of Hydraulic Fractures in Rocks," *Society of Petroleum Engineers Journal*, Vol. 7, p. 310, 1967.

Haimson, B., "Hydraulic Fracture in Porous and Nonporous Rock and its Potential for Determining *In Situ* Stress at Great Depth," *Ph.D. Thesis*, University of Minnesota, July, 1968.

Haimson, B., LaComb, J., Jones, A. H. and Green, S. J., "Deep Stress Measurements in Tuff at the Nevada Test Site," *Terra Tek Report* TR 74-11, January, 1974.

Hussain, M. A., Pu, S. L. and Underwood, J., "Strain-Energy Release Rate for a Crack Under Combined Mode I and Mode II," *Fracture Analysis*, Proc. of the 1973 National Symposium on Fracture Mechanics, Part II, ASTM, STP 560, p. 2, 1974.

Hubbert, M. K. and Willis, B. G., "Mechanics of Hydraulic Fracturing," *Trans. Soc. Petr. Eng.*, Vol. 210, p. 153, 1957.

Ingraffea, A. R. and Heuze, F. E., "Fracture Propagation in Rock: Laboratory Tests and Finite Element Analysis," *Site Characterization*, Proc. of the 17th U. S. Symposium on Rock Mechanics, paper 5C4, 1976.

Irwin, G. R., "Analysis of Stresses and Strains Near the End of a Crack Transversing a Plate," *J. Appl. Mech.*, Vol. 24, p. 361, 1957.

Irwin, G. R., "Fracture Mechanics," in Structural Mechanics, J. N. Goodier and N. J. Hoff Editors, p. 557, Pergamon Press, N. Y., 1960.

Johnson, J. N., Clifton, R. J., Simonson, E. R. and Green, S. J., "Analysis of Fracture for Hollow Cylindrical and Spherical Rock Specimens Subjected to Internal Pressure with Applications to Underground Nuclear Containment," *Terra Tek Report* TR 73-50, September, 1973.

Kehle, R. O., "The Determination of Tectonic Stresses Through Analysis of Hydraulic Well-Fracturing," *J. Geophys. Res.*, Vol. 69, p. 1964.

Komar, C. A., "ERDA Research in Fracture Technology," Proceedings of ERDA Symposium on Enhanced Oil and Gas REcovery, Vol. 2, paper C1, 1976a.

Komar, C. A., Private Correspondence, Energy Research and Development Administration, (Morgantown Laboratories), 1976b.

Lamont, N. and Jessen, F. W., "The Effects of Existing Fractures in Rock on the Extension of Hydraulic Fractures," *J. of Petr. Tech.*, Vol. 15, p. 1963.

Overbey, W. K., Jr. and Rough, R. L., "Surface Joint Patterns Predict Well-Bore Fracture Orientation," *Oil and Gas Journal*, Vol. 66, p. 84, 1968.

Overbey, W. K., Jr. and Rough, R. L., "Prediction of Oil- and Gas-Bearing Rock Fractures From Surface Structural Features," *U. S. Bureau of Mines Report*, Inv. 7500, p. 14, 1971.

Paris, P. C. and Sih, G. C., "Stress Analysis of Cracks," in Fracture Toughness Testing and Its Application, ASTM, STP 381, p. 30, 1965.

Randolph, P. L., "MHF Research in Green River Basin," Proceedings of the Symposium on Stimulation of Low Permeability Reservoirs, Colorado School of Mines, February, 1976.

Raleigh, C. B., Healy, J. H. and Bredehoeft, J. D., "Faulting and Crustal Stress at Rangely, Colorado," Flow and Fracture of Rock, The Griggs Volume, Geophysical Monograph Series of the American Geophysical Union, Washington, D. C., p. 275, 1972.

Rice, J. R. and Levy, N., "The Part-Through Surface Crack in an Elastic Plate," *Brown University Technical Report* No. NASA NGL 40-002-Q8013 to the National Aeronautics and Space Administration, 1970.

Rice, J. R., "Mathematical Analysis in the Mechanics of Fracture," in Treatise on Fracture, Vol. II, Ch. 3, H. Liebowitz editor, Academic Press, 1968.

Rough, R. L. and Lambert, W. G., "*In Situ* Strain Orientations: A Comparison of Three Measuring Techniques," *U. S. Bureau of Mines Report*, Inv. 7575, p. 17, 1971.

Sbar, M. L. and Sykes, L. R., "Contemporary Compressive Stress and Seismicity in Eastern North America: An Example of Intra-Plate Tectonics," *Geological Society of America Bulletin*, Vol. 84, p. 1861, 1973.

Sellers, J. B., "Strain Relief Overcoring to Measure *In Situ* Stress," *U. S. Army Corps Engineers Report*, Buffalo District, N. Y., p. 23, 1969.

Sneddon, I. N., "The Distribution of Stress in the Neighborhood of a Crack in an Elastic Solid," Proceedings, Royal Soc. London, Series A, Vol. 187, p. 229, 1946.

Smith, E., Private Communication, Columbia Gas System Service Corporation, 1976.

Swolfs, H., Lingle, R. and Thomas, J., "Strain Relaxation Tests on Selected Cores from Columbia Gas System Service Corporation Well No. 20402, Lincoln County, West Virginia," *Terra Tek Technical Report* TR 76-60, November, 1976.

Underwood, J. H., "Stress-Intensity Factors for Internally Pressurized Thick-Walled Cylinders," STP 513, ASTM, p. 59, 1972.

Wroble, J. L., Private Communication, Pacific Transmission Supply Company, 1976.

This page intentionally left blank.

APPENDIX

Description of Laboratory Tests

The Fracture-Toughness Burst Test

The experiment used to determine a materials resistance to fracture extension consists of subjecting a prenotched, thick-walled cylinder to an internal pressure that loads the wall at the inner radius but does not load the faces of the notch. This type of test has been proposed by Clifton, *et al.*, (1976) to measure the critical stress intensity factor K_{Ic}, of geologic materials. The experimental configuration is shown in Figure A2. The test specimen is a thick-walled cylinder with an outer-to-inner-diameter ratio of 10 or more. Two radially opposed prenotches are cut into the inner bore and penetrate one tenth of the wall thickness along the full length of the specimen. Prenotching is accomplished using a diamond-impregnated copper wire, 0.2 mm (0.008 in.) in diameter. A soft impermeable jacket of urethane tubing with a thickness of .15 mm (0.060 in.) prevents the fluid pressure from loading the crack faces and the fluid from permeating the rock matrix. The jacket extends into steel end caps that are attached to each end of the sample. The seal for the pressurizing fluid is made in the steel end caps as shown in Figure A2. A cone shaped rubber plug forms a seal between the inside of the urethane jacket and the fluid port when a small axial force is applied to the system. The seal pressure is varied by changing the amount of interference between the steel end cap and the compression rod. A small steel tube in the upper rubber end seal, allows fluid to communicate between the inner bore and the high pressure line.

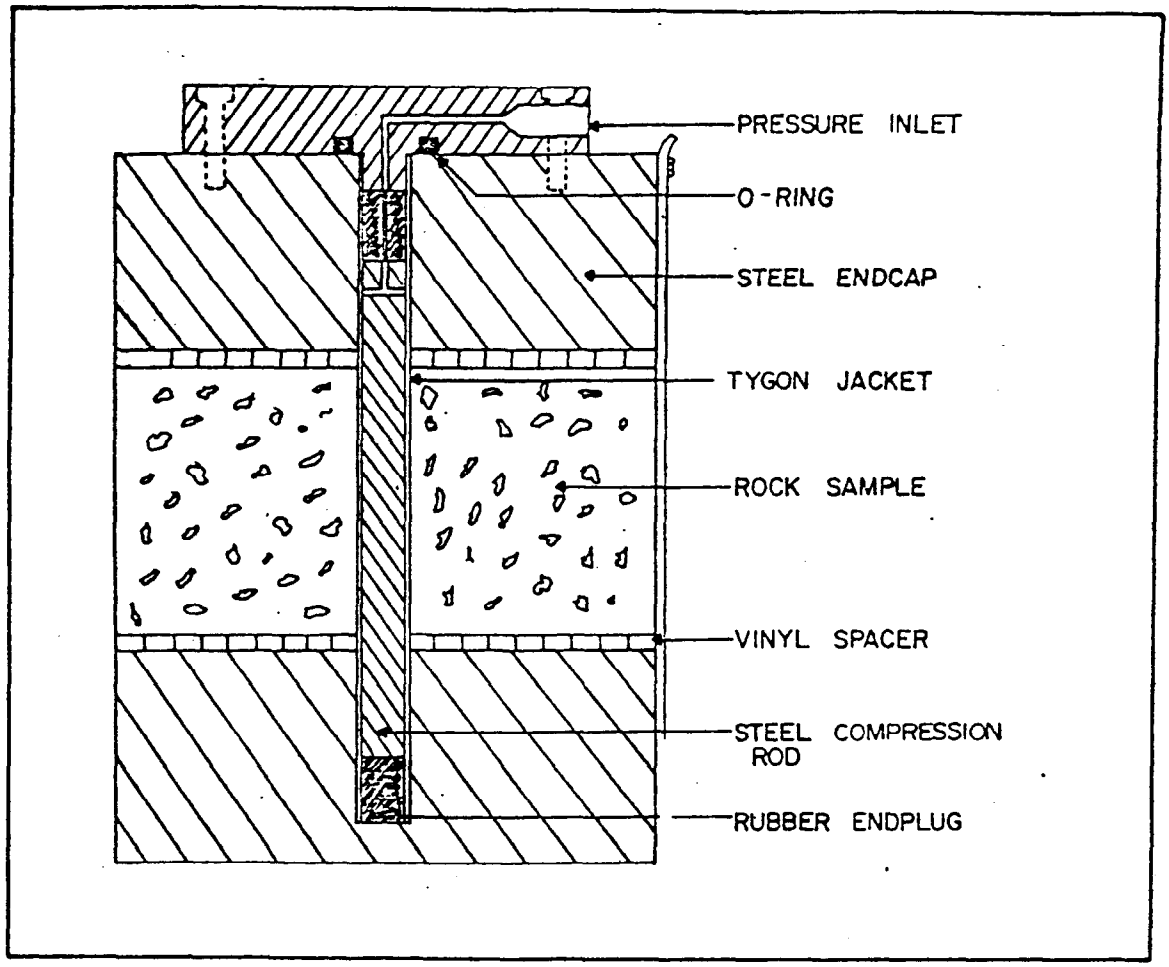

Figure A1. Cross-section of a typical specimen for fracture-toughness-burst test.

To evaluate K_{Ic} for a given sample material the internal pressure is increased slowly and recorded until a crack is observed to propagate. As predicted by the analysis of this configuration (Bowie and Freese, 1970) the first phase of crack propagation is stable for wall-thickness ratio greater than 10. Further increase of the internal pressure initiates unstable crack growth and results in catastrophic failure of the cylindrical specimen. The maximum Internal pressure (P_i) that can be applied to the inner wall is related to the critical intensity factor, K_{Ic}, of the

tested material and the geometry of the sample, by the following equation:

$$K_{Ic} = K^*_{Ic} \ (P_i \sqrt{\pi a})$$

where a is the internal radius and K^*_{Ic} corresponds to the local minimum value of the numerically calculated function K^*_I shown in Figures A2 and A3 for different wall thickness ratios, w, and crack geometry. For example, for a wall thickness ratio of 10, K^*_{Ic} is given by 0.245 or 0.42 depending on whether the sample has a single or double radial cracks, respectively.

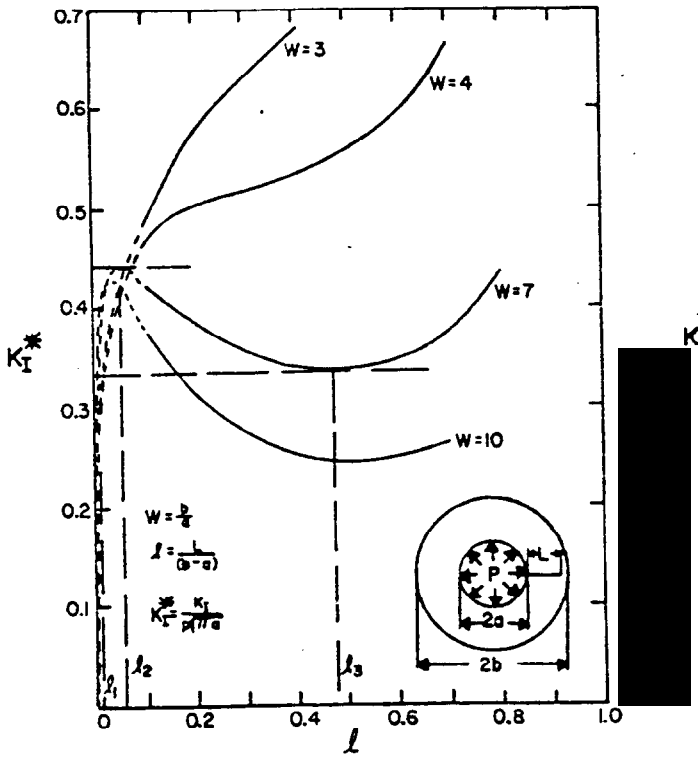

Figure A2. Stress-intensity factor for jacketed cylinder with one radial crack (from Bowie and Freese, 1972).

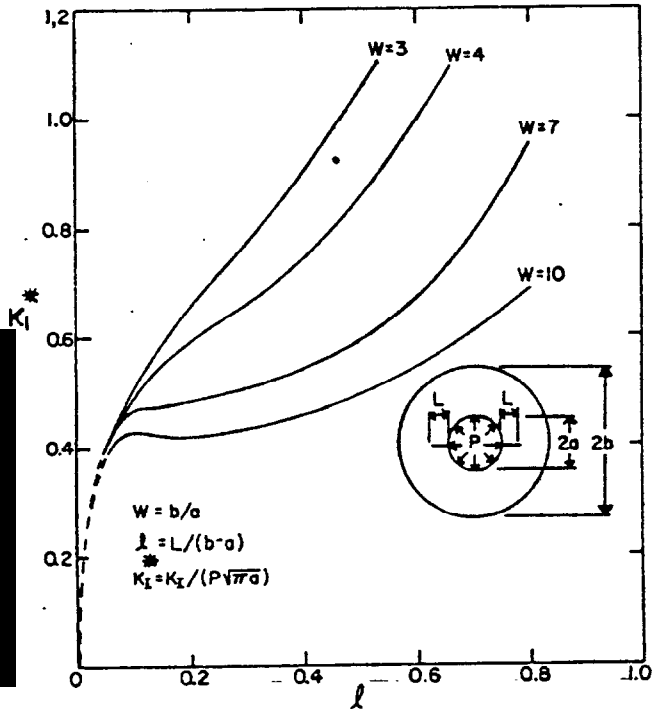

Figure A3. Stress-intensity factor for jacketed cylinder with two radial cracks (from Bowie and Freese, 1972).

Results of Fracture Toughness Tests

The results of the fracture toughness tests are further evidence of the anisotropic nature of this shale (see Table A1). Figures A4 and A5 are

TABLE AI

Results of Fracture Toughness Tests

Sample Depth m (ft.)	b/a w	P_i Failure Pressure MPa (psi)	K_{IC}*	K_{IC} MPa$\sqrt{m}$ (psi$\sqrt{in}$)	Remarks
826.5 (2711)	10.47	19.5 (2825)	0.4	42.4 (1220)	Failure initiated along notch then turned along pre-existing fracture
839 (2761)	10.47	26.21 (3800)	0.25	38.2 (1100)	Failure ignored notch and occurred on a pre-existing fracture

photographs of the two samples that were pre-notched and pressurized with impermeable membranes. In Figure A4 the failure plane originated at the tips of the pre-notch but turned the moment it intersected a natural fracture. The failure plane in Figure A5 began in three places, at one pre-notch and at radially opposed points along a natural fracture, however, catastrophic failure occurred along the natural fracture.

TABLE A2

Tabulation of Functions F and G (Paris and Sih, 1965)

	One Radial Crack		Two Radial Cracks	
L/a	F(L/a)	G(L/a)	F(L/a)	G(L/a)
0.00	2.26	3.39	2.26	3.39
0.10	1.98	2.73	2.06	2.93
0.20	1.82	2.30	1.83	2.41
0.30	1.69	2.04	1.70	2.15
0.40	1.58	1.86	1.61	1.96
0.50	1.49	1.73	1.57	1.83
0.60	1.42	1.64	1.52	1.71
0.80	1.32	1.47	1.43	1.58
1.00	1.22	1.37	1.38	1.45
1.50	1.06	1.18	1.26	1.29
2.00	1.01	1.06	1.20	1.21
3.00	0.93	0.94	1.13	1.14
5.00	0.81	0.81	1.06	1.07
10.00	0.75	0.75	1.03	1.03
∞	0.707	0.707	1.00	1.00

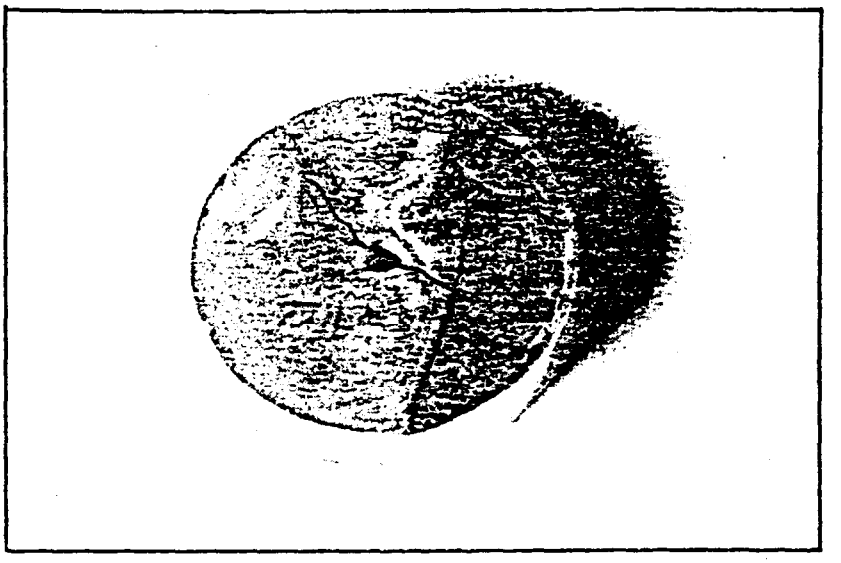

Figure A4. Fracture toughness sample from 826.5 m (2711 ft.)

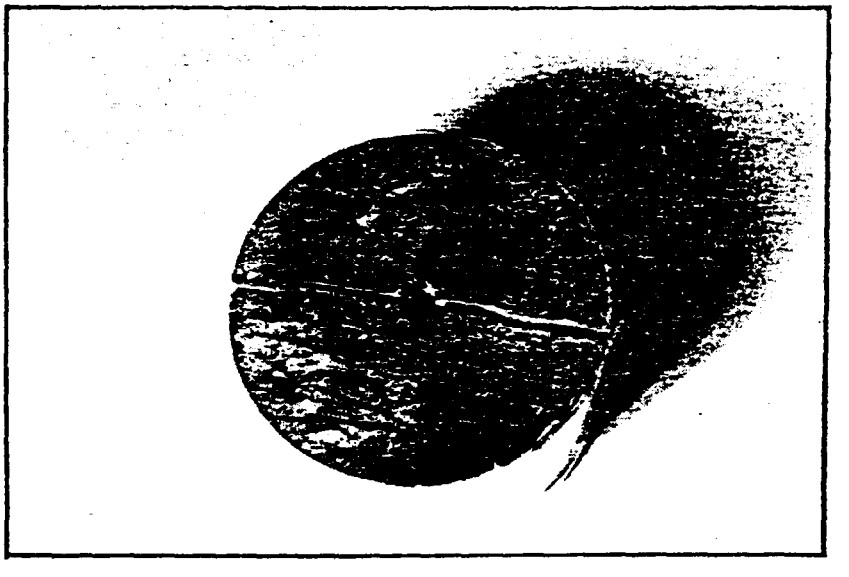

Figure A5. Fracture toughness sample from 829 m (2761 ft.)

This page intentionally left blank.

ACKNOWLEDGMENT

The authors would like to acknowledge the help of Dr. B.C. Haimson, of the University of Wisconsin, Madison, in supervising the field experiment. Helpful discussions with Dr. A.H. Jones and Dr. E.R. Simonson of Terra Tek, and pertinent comments and criticism of many individuals from the oil and gas industry with regard to the first draft of this report made it possible to have the work in its present form.